

Inhibition of Class A β -Lactamase (TEM-1) by Narrow Fractions of Humic Substances

Tatyana A. Mikhnevich, Alexandra V. Vyatkina (Turkova), Vitaly G. Grigorenko, Maya Yu. Rubtsova, Gleb D. Rukhovich, Maria A. Letarova, Darya S. Kravtsova, Sergey A. Vladimirov, Alexey A. Orlov, Evgeny N. Nikolaev, Alexander Zhrebker, and Irina V. Perminova*



Cite This: *ACS Omega* 2021, 6, 23873–23883



Read Online

ACCESS |



Metrics & More

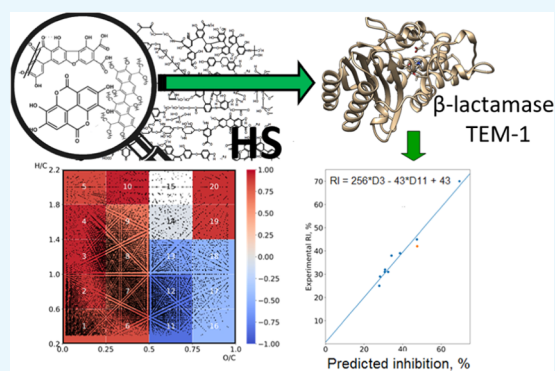


Article Recommendations



Supporting Information

ABSTRACT: Antimicrobial resistance is a global threat. The use of biologically active natural products alone or in combination with the clinically proven antimicrobial agents might be a useful strategy to fight the resistance. The scientific hypotheses of this study were twofold: (1) the natural humic substances rich in dicarboxyl, phenolic, heteroaryl, and other fragments might possess inhibitory activity against β -lactamases, and (2) this inhibitory activity might be linked to the molecular composition of the humic ensemble. To test these hypotheses, we used humic substances (HS) from different sources (coal, peat, and soil) and of different fractional compositions (humic acids, humatmelanic acids, and narrow fractions from solid-phase extraction) for inhibiting serine β -lactamase TEM-1. Fourier transform ion cyclotron resonance mass spectrometry (FTICR MS) was used to characterize the molecular composition of all humic materials used in this study. The kinetic assay with chromogenic substrate CENTA was used for assessment of inhibitory activity. The inhibition data have shown that among all humic materials tested, a distinct activity was observed within apolar fractions of humatmelanic acid isolated from lignite. The decrease in the hydrolysis rate in the presence of most active fractions was 42% (with sulbactam—87%). Of particular importance is that these very fractions caused a synergistic effect (2-fold) for the combinations with sulbactam. Linking the observed inhibition effects to molecular composition revealed the preferential contribution of low-oxidized aromatic and acyclic components such as flavonoid-, lignin, and terpenoid-like molecules. The binding of single low-molecular-weight components to the cryptic allosteric site along with supramolecular interactions of humic aggregates with the protein surface could be considered as a major contributor to the observed inhibition. We believe that fine fractionation of hydrophobic humic materials along with molecular modeling studies on the interaction between humic molecules and β -lactamases might contribute to the development of novel β -lactamase inhibitors of humic nature.



INTRODUCTION

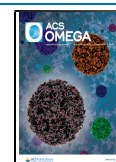
Antimicrobial resistance is a serious threat to global health.^{1,2} β -Lactam antibiotics (penicillins, cephalosporins, carbapenems, and monobactams) are the ones most widely used in clinical practice.^{3,4} The major mechanism of bacterial resistance to these antibiotics is production of hydrolytic enzymes- β -lactamases (EC 3.5.2.6).⁵ These bacterial enzymes are represented by a superfamily of about 2800 variants with class A serine β -lactamases belonging to the most common clinical pathogens. The competitive β -lactam inhibitors (sulbactam, tazobactam, and clavulanic acid) are widely used to suppress the activity of β -lactamases. They produce a stable covalent bond with the serine residue in the active site of the enzyme. This mechanism of β -lactamase inhibition is well understood, and currently, co-administration of susceptible β -lactams with the covalent inhibitors (e.g., clavulanate and sulbactam) is a proven therapeutic strategy.⁶ However, bacteria evolved through mutations of the key amino acid residues, which brought

about a change in the structure of β -lactamases providing for resistance to both antibiotics and β -lactam inhibitors.^{6,7} This mutational variability is primarily characteristic of class A of the serine β -lactamases, in particular, of the TEM-type enzymes.^{8,9} As a result, substantial efforts were directed over the last years on understanding the conformational behavior of β -lactamase, which can be relevant to allosteric inhibition—a viable alternative for drug design.^{10–13} An allosteric binding site for TEM-1 was first reported by Horn and Shoichert,¹⁴ who suggested that the movement of H10 helix away from the protein core enables binding of allosteric inhibitors to a

Received: May 31, 2021

Accepted: August 25, 2021

Published: September 7, 2021



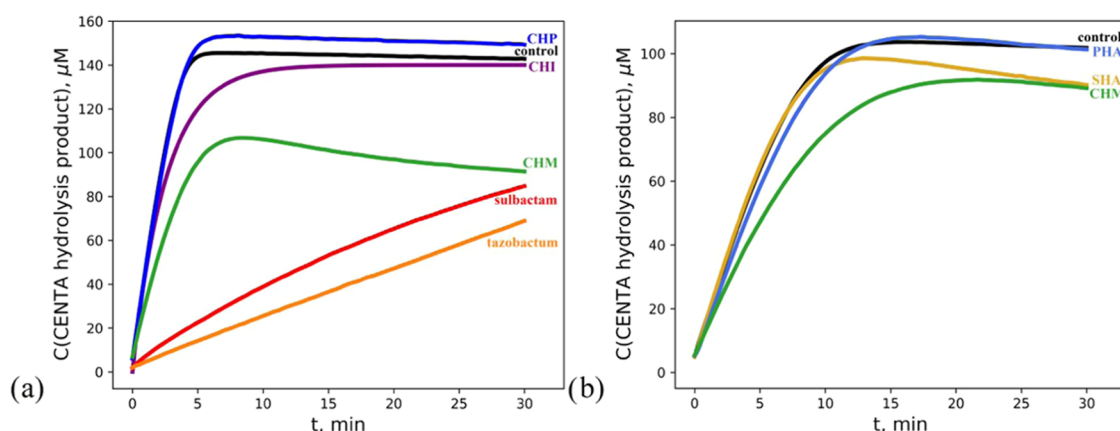


Figure 1. Inhibition curves of β -lactamase TEM-1 by humic materials from different sources (highlighted in colors): (a) coal humic acids (CHP—blue, CHI—purple) and coal hymatomelanic acids (CHM—green), control (black), sulbactam (red), tazobactam (orange); (b) peat HA (PHA—light blue), soil HA (SHA—gold), and coal hymatomelanic acid (CHM—green). Concentrations of humic materials— $50 \text{ mg}\cdot\text{L}^{-1}$, sulbactam and tazobactam—5 and $0.5 \text{ }\mu\text{M}$, respectively. Substrate—CENTA ($100 \text{ }\mu\text{M}$); concentration of TEM-1: 17 nM (a) and 10 nM (b).

hydrophobic pocket formed by the two helices H10 and H11 on one side and the β -sheet composed of $\beta 3$, $\beta 4$, and $\beta 5$ on the other side. However, the allosteric inhibition strategies are much less well explored, while structural communication that leads to inhibition of enzyme activity is not well understood.¹⁵ The same is true for the inhibitory activity of small-molecule aggregates (“colloidal inhibitors”), which block β -lactamase activity by orchestrated conformation changes in the active center.¹⁶

Despite the much less understanding of the mechanism of allosteric inhibition as well as “colloidal inhibition” by molecular aggregates, they still offer new opportunities for a search of molecules capable of bringing about a reduction in the catalytic activity of β -lactamases. Moreover, these alternative inhibitors could work synergistically with traditional inhibitors, which makes this strategy even more attractive. The search for allosteric inhibitors of β -lactamases was conducted using both X-ray crystallographic studies with experimental ligands^{14,17,18} and theoretical studies on molecular modeling and screening of chemical libraries.¹⁵ The reports on small-molecule aggregates also considered synthetic compounds. While reviewing these efforts, we could not find a single report on both experimental and theoretical screening of natural compounds. At the same time, the use of natural compounds alone or in combination with the clinically proven agents might be a useful strategy to fight resistance. In this regard, of particular interest are natural humic substances (HS). They represent complex molecular systems comprising both low- and high-molecular-weight biomolecular precursors. The structural fragments present in HS molecules include dicarboxylic aromatic acids, phenols, N-heteroaryls, peptides, sugars, etc.¹⁹ This might indicate good prospects of HS for noncovalent binding to β -lactamases. On the other side, they are capable of producing aggregates in solution, which could lead to aggregate–enzyme interactions.²⁰ In the literature, numerous reports exist on HS capability for binding to various proteins, including enzymes.^{20–24} Of particular importance is the recent patent on the inhibitory activity of the low-molecular-weight synthetic HS with respect to β -lactamase.²⁵ At the same time, we have not found similar reports for natural HS in both open and patent literature.

The objective of this study was to test the capabilities of natural HS from different sources and of different fractional compositions for inhibition of β -lactamases. We used three major commercially relevant sources of HS (coal, peat, and soil),

and ran experiments both on broad traditional fractions such as alkali-soluble humic acids (HA) and ethanol-soluble hymatomelanic acids (HMA), and on narrow fractions obtained from use of solid-phase extraction (SPE) and the gradient elution technique. Serine β -lactamase of class A—TEM-1—was used as a model enzyme. Both inhibitory activity and the synergistic effects of HS were studied using combinations with sulbactam and tazobactam.

RESULTS AND DISCUSSION

Assessment of the Inhibitory Activity of Humic Materials with Respect to β -Lactamase TEM-1. The inhibitory activity of humic materials from different sources (coal, peat, and soil) and of different fractional compositions (humic acids, hymatomelanic acids, and narrow SPE fractions) towards the β -lactamase TEM-1 was investigated using kinetic assays. Well-known β -lactam inhibitors of class A β -lactamases—sulbactam and tazobactam—were used as positive controls. The experiments on the inhibitory activity of HS from different sources were conducted at two different concentrations of enzyme (17 and 10 nM, respectively). The obtained results are given in Figure 1a,b, respectively.

Among the common humic alkali isolates from different sources (CHI, CHP, SHA, and PHA), a slight inhibitory activity was observed only for coal humic acids isolated from lignite (CHI). At the same time, a very distinct activity was observed for the ethanol-soluble fraction of coal humic acid (CHM), which caused a reduction of 42% in the catalytic activity of TEM-1. The corresponding RI values for sulbactam and tazobactam were 88 and 93%, respectively.

This motivated us to undertake further separation of the CHM sample into narrow fractions differing in polarity. This was done by gradient elution with water:methanol solutions with increasing content of methanol (the isolation details are given in the Experimental Section). The obtained nine fractions were designated by the indices corresponding to the concentration of methanol in the solution. They were isolated as solid materials and used for the bioassays under the same conditions with a TEM-1 concentration of 17 nM. The data are shown in Figure 2 (some data are omitted to avoid overlap of the curves. All data are shown in Figure S3 in the SI.)

It can be seen that all narrow fractions of CHM showed inhibitory activity. Of particular importance is that the inhibitory

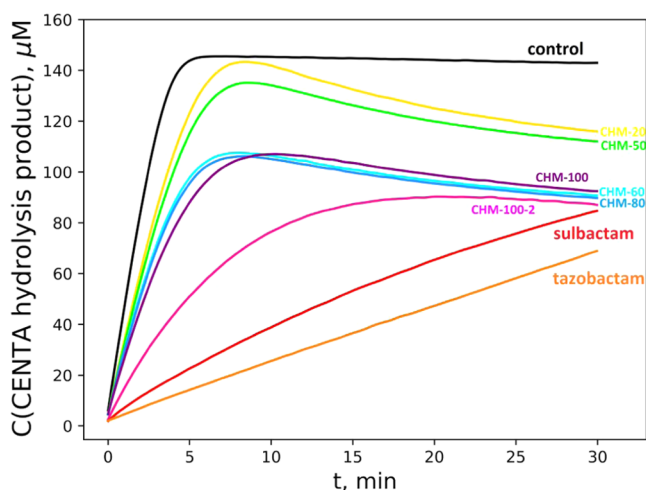


Figure 2. Inhibition of β -lactamase TEM-1 by the narrow fractions of humic materials (highlighted in colors): CHM-20 (yellow), CHM-50 (lime), CHM-60 (cyan), CHM-80 (light blue), CHM-100-1 (purple), and CHM-100-2 (pink); control (black), sulbactam (red), tazobactam (orange). Concentrations of humic materials—50 $\text{mg}\cdot\text{L}^{-1}$, sulbactam and tazobactam—5 and 0.5 μM , respectively. Substrate—CENTA (100 μM); concentration of TEM-1: 17 nM.

activity increased along with an increase in methanol content of the eluate, which is indicative of the less polar and more hydrophobic character of the corresponding humic material. For quantitative assessment of the inhibitory activity of the fractions, the values of the relative decrease in initial hydrolysis rate RI were calculated according to eq 1 and are summarized in Table 1.

Table 1. Initial Rates (v_2) and Relative Decrease in the Initial Rate (RI, %) of CENTA Hydrolysis by β -Lactamase TEM-1 in the Presence of CHM Fractions^a

CHM fraction	v_2 ($\mu\text{M}\cdot\text{s}^{-1}$)	RI (%)
CHM-10	0.43 ± 0.02	31.5 ± 1.5
CHM-20	0.45 ± 0.03	26.8 ± 1.8
CHM-30	0.43 ± 0.02	30.1 ± 1.4
CHM-40	0.41 ± 0.02	33.3 ± 1.6
CHM-50	0.42 ± 0.02	31.9 ± 1.5
CHM-60	0.38 ± 0.02	39.4 ± 2.1
CHM-80	0.36 ± 0.02	41.3 ± 2.5
CHM-100-1	0.32 ± 0.02	47.7 ± 3.0
CHM-100-2	0.18 ± 0.01	70.8 ± 3.9
CHM-parent	0.36 ± 0.02	41.9 ± 2.3

^aRI was determined as described in the Experimental Section.

The highest inhibitory activity was reached in the most hydrophobic fraction CHM-100-2, which was obtained by the second pure methanol elution of the PPL SPE cartridge. The CHM-100-1, CHM-80, and CHM-60 samples slightly exceeded the parent CHM in inhibitory activity. At the same time, the more hydrophilic fractions, which were eluted with more polar eluents, nominally CHM-50, CHM-40, CHM-30, CHM-20, and CHM-10, inhibited β -lactamase to a lesser extent as compared to the parent humic material—CHM. The obtained data corroborate well our previous finding on the antiviral properties of HS that the more hydrophobic humic materials exhibited a higher biological activity.

Inhibitory Activity of the Combinations of the Humic Fractions with β -Lactam Inhibitors. As the next step of this study, the possible synergy between the humic and β -lactam inhibitors (sulbactam and tazobactam) was assessed. For this purpose, we performed the kinetic experiments on CENTA hydrolysis by β -lactamase TEM-1 in the presence of both sulbactam and tazobactam and four types of humic inhibitors. The latter included the CHM sample and its three hydrophobic fractions with the highest inhibitory activity: CHM-50, CHM-100-1, and CHM-100-2. The corresponding kinetic curves are shown in Figure 3.

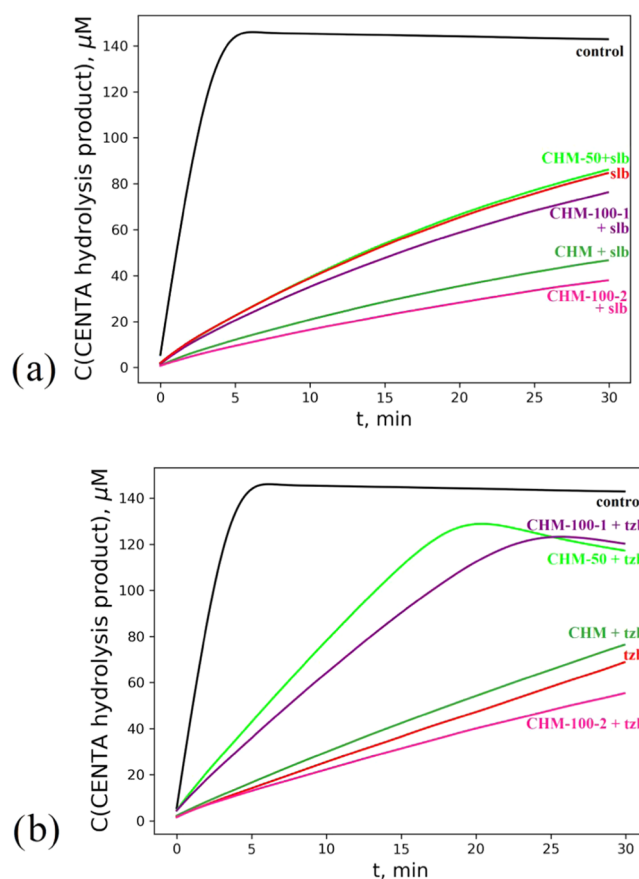


Figure 3. Inhibition of β -lactamase TEM-1 in the presence of combinations of β -lactam and humic inhibitors: (a) 5 μM sulbactam and (b) 0.5 μM tazobactam, humic inhibitors (50 $\text{mg}\cdot\text{L}^{-1}$). Combinations of β -lactam and humic inhibitors are highlighted in green (CHM), lime (CHM-50), purple (CHM-100-1), pink (CHM-100-2), red (β -lactam inhibitor alone), and black (control without inhibitors).

In the case of sulbactam, its combination with all humic fractions (except for CHM-50) caused enhanced inhibition of β -lactamase as compared to the individual effect of sulbactam (Figure 3a). The largest effect was observed for the combination of sulbactam with the most hydrophobic fraction CHM-100-2, which was closely followed by combinations with the parent humic material—CHM. At the same time, for tazobactam, a much less profound enhancement of the inhibitory effect was observed only in the case of CHM-100-2. CHM did not cause any change in tazobactam activity, whereas CHM-50 and CHM-100 caused a slight decrease in the inhibitory effect of tazobactam (Figure 3b).

To explore if the observed inhibitory effect of the combinations of sulbactam with the humic materials used in this study is additive or synergistic, we used the additive model (eq 2) developed by Chou and Talalay for the combined action of several competitive inhibitors.²⁶ The initial velocity of the uninhibited reaction (v_0) was $0.62 \pm 0.04 \mu\text{M}\cdot\text{s}^{-1}$, and the initial velocity in the presence of the β -lactam inhibitor (v_1) was $0.070 \pm 0.005 \mu\text{M}\cdot\text{s}^{-1}$ for sulbactam, and $0.040 \pm 0.003 \mu\text{M}\cdot\text{s}^{-1}$ for tazobactam. The calculated results for the experimental and simulated initial velocities are given in Table 2, where v_2 is the

Table 2. Experimental and Calculated Initial Velocities of the Hydrolysis Reaction ($\mu\text{M}\cdot\text{s}^{-1}$)

HS sample	sulbactam		tazobactam	
	$v_{1,2 \text{ exp.}} \times 10^{-2a}$	$v_{1,2 \text{ calc.}} \times 10^{-2b}$	$v_{1,2 \text{ exp.}} \times 10^{-2}$	$v_{1,2 \text{ calc.}} \times 10^{-2}$
none	7.0 ± 0.5		4.0 ± 0.3	
CHM	4.0 ± 0.3	6.7	4.9 ± 0.4	4.0
CHM-50	7.4 ± 0.5	6.9	13.0 ± 0.9	4.0
CHM-100-1	6.8 ± 0.4	6.6	10.7 ± 0.8	3.9
CHM-100-2	3.2 ± 0.2	5.7	3.9 ± 0.3	3.6

^aExp, experimental. ^bCalc, calculated using eq 2.

initial velocity of the reaction in the presence of inhibitor 2 (HS) only, $v_{1,2}$ is the initial velocity of the reaction in the presence of both humic and β -lactam inhibitors. The data obtained show that in case of the combinations of sulbactam with CHM and

CHM-100-2, the experimental initial velocities were lesser as compared to the calculated additive ones. This is indicative of the synergistic effect exerted by the humic inhibitors on sulbactam. In case of the combinations of sulbactam with CHM-50 and CHM-100, the inhibition rates were equal to the sum of individual reaction rates for sulbactam and for the CHM fractions. This is indicative of additive effects. In the case of tazobactam, CHM-100-2 showed an additive effect, whereas CHM, CHM-50, and CHM-100-1 showed antagonistic effects.

We assumed that the inconsistency of the effects observed might stem from the interaction of some individual HS components with the enzyme, which affected the binding of inhibitors in the active center. It should be noted that sulbactam has a substantially smaller longitudinal size as compared to tazobactam. Along with that, the reported data on molecular dynamics modeling demonstrated that a molecule of sulbactam was more mobile in the cavity of the active center and capable of performing rotational movements while remaining bound to the enzyme.²⁷ Thus, binding of humic molecular components with the allosteric centers of the protein could affect the conformation of the active site of β -lactamase and contribute to formation of its more stable complex with sulbactam.

Correlation and Regression Analysis of the Molecular Composition and Inhibitory Activity of the Narrow CHM Fractions. For linking the observed inhibitory activity to the molecular components present in the narrow CHM fractions, all fractions were characterized using high-resolution Fourier

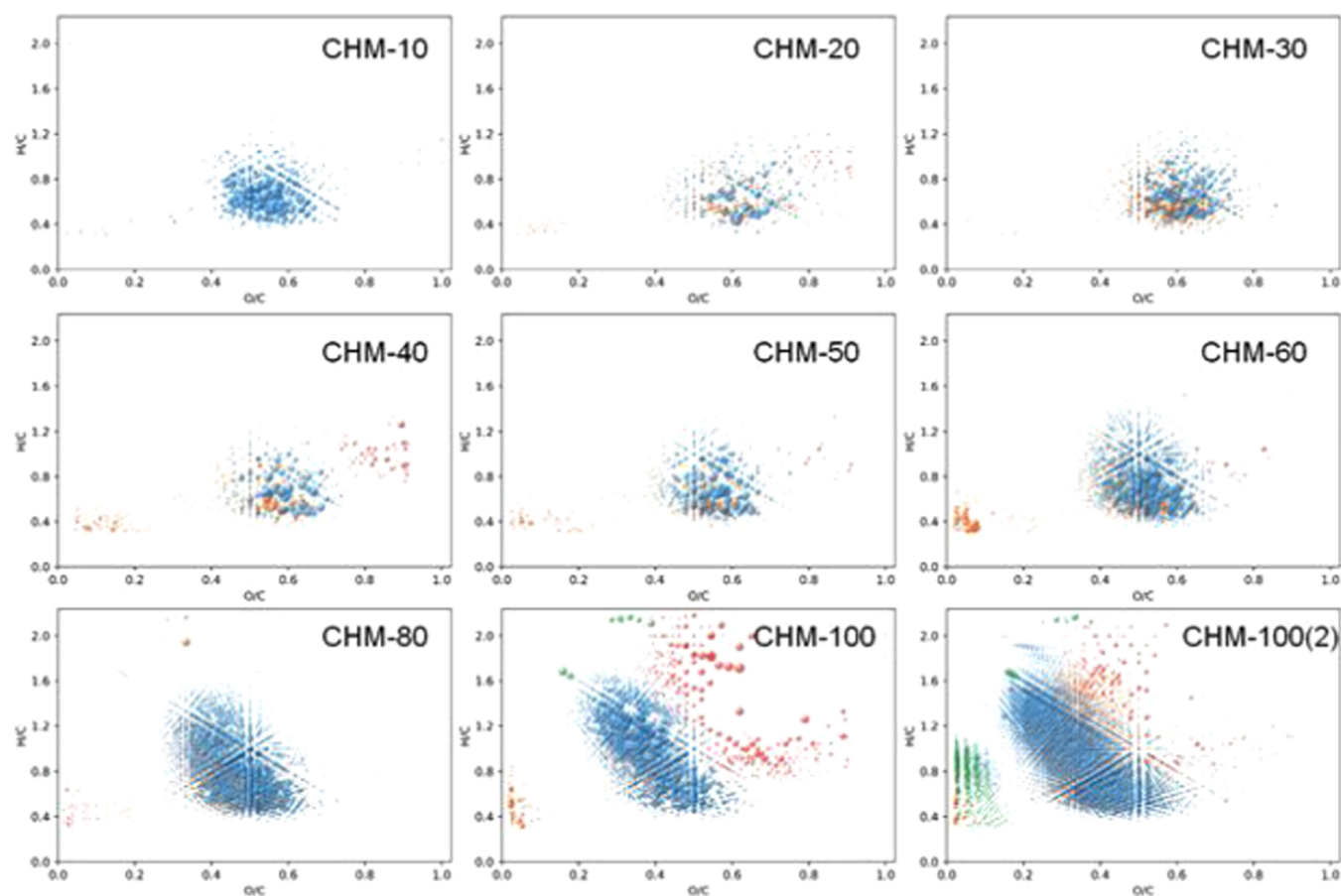


Figure 4. van Krevelen diagrams of the narrow CHM fractions differing in polarity obtained by elution from the SPE PPL cartridges using $\text{CH}_3\text{OH}:\text{H}_2\text{O}$ mixtures. The methanol proportion is designated in the legend. CHO formulae are highlighted in blue, CHON in yellow, CHOS in green, and CHONS in red. The dot size corresponds to the peak intensity in the mass list.

transform ion cyclotron resonance mass spectrometry (FTICR MS). The corresponding data are shown in Figure 4 as van Krevelen diagrams plotted from molecular formulae assigned to the obtained FTICR MS data.

It can be seen that the most striking differences between the most nonpolar (hydrophobic) fractions and the hydrophilic fractions are observed in the content of low-oxidized condensed aromatic compounds and lignin-like species occupying the range with the same O/C values ($O/C < 0.5$) and different H/C values ($H/C < 1$ and $1.0 < H/C < 1.4$), respectively. The fractions eluted with the mixtures containing more than 80% methanol were characterized with a higher contribution of low-oxidized compounds. This is consistent with their hydrophobic character. The number of unique formulae present in each fraction is given in Table 3 (the term “unique” refers to components that could be found only in this fraction and could not be observed in the others).

Table 3. Number of Total and Unique Formulae Determined in the Narrow CHM Fractions

fraction	total	unique	fraction	total	unique
CHM-parent	4306	0	CHM-50	1259	288
CHM-10	428	49	CHM-60	1915	261
CHM-20	1036	231	CHM-80	3013	489
CHM-30	1406	330	CHM-100-1	2365	442
CHM-40	1009	261	CHM-100-2	5365	1925

Molecular compositions of the fractions varied substantially in chemical diversity. The first five fractions (the most polar ones) had the least number of constituents (Table 4). This might be attributed to the lower ionization efficiency of the polar components as compared to the hydrophobic ones.²⁸ The four more hydrophobic fractions were characterized with a higher number of constituents. This could be a result of resolving the charge-combating issue in the ion cyclotron resonance (ICR) detector.^{29,30} As a total, fractionation revealed

4276 new molecular compositions that could not be observed in the parent CHM material. This could be caused by the charge competition and slight selectivity of electrospray ionization (ESI) taking place during the FTICR MS analysis.^{29,30} At the same time, the molecular constituents found in the CHM fractions covered all formulae determined in the parent CHM material.

For establishing the relationship between the molecular composition and inhibitory activity of the CHM fractions, we generated quantitative descriptors as described by Perminova.³¹ In brief, we binned the whole field of each van Krevelen diagram shown in Figure 4 in the range of H/C values from 0.2 to 2.2 and of O/C values from 0 to 1 into 20 cells as shown in Figure 5, and calculated the occupation density of each cell.³¹ The obtained values were designated with a capital D followed by the sequential number of the cell (Table 4).

The maximum differences in the molecular compositions of the hydrophobic (eluted with methanol content >50%) and hydrophilic (eluted with methanol content <50%) fractions were observed for the descriptors related to the contributions of the condensed, lignin-like, and terpenoid compounds (D3, D6, and D7) and those related to oxidized aromatic tannins (D11, D12). The highest values of the former and the lowest values of the latter were observed in the most hydrophobic (and the most active) fractions. The obtained structural descriptors were used in combination with the inhibitory activity data set (Table 1) for correlation–regression analysis. The results are presented in Figure 5.

Red color highlights direct correlations between the molecular components of the CHM fractions occupying these cells and their inhibitory activity, whereas blue color indicates inverse correlations. The correlation coefficient (*R* value) is given as a color-coded bar in Figure 5a. The black dots in the van Krevelen diagram represent all formulae that been seen in the nine CHM fractions. The dot size is proportional to the number of compounds with the same formulae in the different fractions. The constructed integral van Krevelen diagram gives a much

Table 4. Descriptors of Molecular Compositions of the CHM Fractions Calculated from the Occupation Density of the Corresponding van Krevelen Diagrams

	CHM-10	CHM-20	CHM-30	CHM-40	CHM-50	CHM-60	CHM-80	CHM-100	CHM-100_2
D1	0.006	0	0	0.003	0.001	0.001	0.001	0.003	0.011
D2	0	0	0	0.001	0	0	0	0.002	0.083
D3	0	0	0	0	0	0	0	0.023	0.107
D4	0	0	0	0	0	0	0	0.009	0.044
D5	0.002	0	0	0	0	0	0	0	0.007
D6	0.065	0.024	0.013	0.022	0.02	0.046	0.068	0.076	0.099
D7	0.146	0.04	0.022	0.052	0.084	0.215	0.35	0.304	0.293
D8	0.006	0.001	0.002	0.008	0.019	0.061	0.214	0.383	0.211
D9	0	0	0	0	0	0.002	0.017	0.078	0.044
D10	0	0	0	0	0	0	0	0.001	0.003
D11	0.289	0.357	0.348	0.286	0.249	0.209	0.107	0.041	0.028
D12	0.46	0.46	0.534	0.559	0.563	0.398	0.204	0.065	0.041
D13	0.019	0.04	0.049	0.065	0.059	0.064	0.037	0.011	0.008
D14	0	0	0	0	0.001	0.002	0.002	0	0
D15	0	0	0	0	0	0	0	0	0
D16	0.001	0.024	0.01	0	0.001	0	0	0	0
D17	0.003	0.048	0.019	0.002	0.003	0.001	0	0	0.001
D18	0.001	0.008	0.003	0.001	0	0	0	0	0
D19	0	0	0	0	0	0	0	0	0.002
D20	0	0	0	0	0	0	0	0.001	0.012

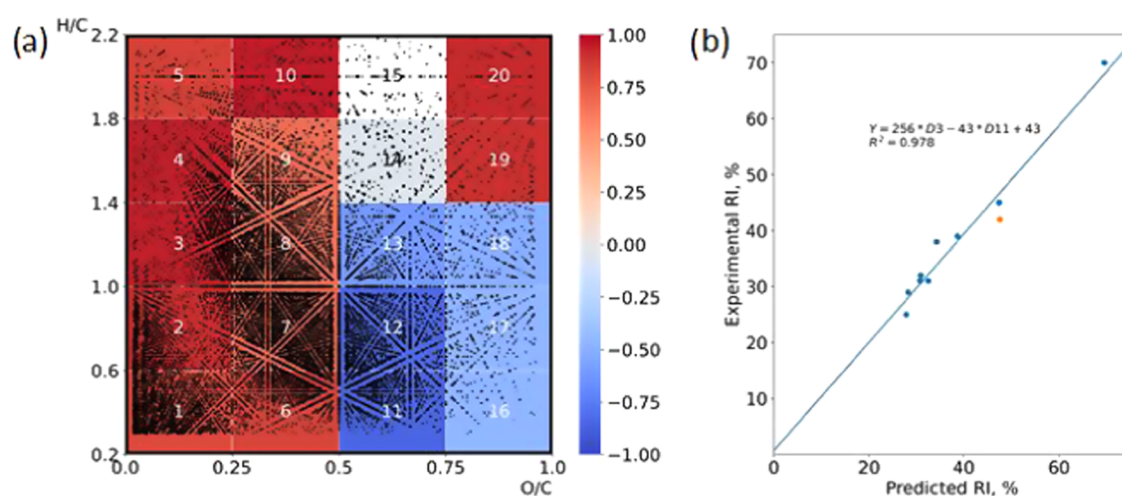


Figure 5. Correlation analysis data (a) and regression analysis data (b) obtained for the sets of descriptors of the occupational density of van Krevelen diagrams (Table 4) and the inhibitory activity of the CHM fractions (Table 1). The colors indicate the values of the correlation coefficient. The regression line corresponds to the equation $RI (\%) = 256 \times D3 - 43 \times D11 + 43$.

better idea of the occupation density distributions of all molecular components, which were measured using FTICR MS in the nine narrow CHM fractions. It can be deduced from Figure 5a that an increase in the inhibitory activity of the CHM fractions (a decrease in the rate of CENTA hydrolysis) is associated with an increase in the contribution of the relatively more hydrophobic components—condensed tannins (D3, D6), unsaturated low-oxidized compounds (D2, D4), lignin-like and terpenoid species (D3, D7), whereas a decrease in activity is associated with an increase in the proportion of the relatively less hydrophobic, more polar oxidized tannins (D11, D12).

The same data set was used for multiple regression analysis in order to develop a regression model for inhibitory activity against β -lactamase TEM-1. Due to the small size of the sample set ($n = 9$), the analysis was limited to a linear combination of no more than three descriptors for increasing the robustness of the obtained relationships. The best fit is shown in Figure 5b ($R^2 = 0.978$). The full outcomes of the regression analysis are summarized in Tables S4–S6 in the SI. The regression equation in Figure 5b is consistent with the highest direct contribution of the relatively hydrophobic phenylisopropanoid structures (D3 descriptor) and inverse contribution of the highly oxidized hydrolyzable tannins (D11) to the inhibitory activity of HS towards the TEM-1 β -lactamase used in this study. For validating the obtained regression relationship, we applied it for calculation of the inhibitory activity of the parent sample—CHM, which was not used for the regression analysis. For this purpose, we calculated the occupational density distribution for the CHM sample and ran the corresponding calculations. The predicted and experimental RI values are shown in Figure 5b with a dot highlighted in orange color. It can be seen that the predicted value is in good agreement with the experimentally determined inhibitory activity of CHM: it lies in the closest proximity of the regression curve calculated for the CHM fractions. This might demonstrate the applicability of the obtained relationship for the class of HS under study. Nominally, it might indicate that the most active molecules in the humic ensemble with regard to inhibition of the TEM-1 β -lactamase belong to the relatively hydrophobic components, supposedly, of phenylisopropanoid, flavonoid, polyphenolic, or other less-oxidized aromatic compounds.

For digging deeper into the nature of the active molecular components of HS, we used the approach reported in our previous work.³² It is based on mining the FTICR MS-derived formulae for the molecular components of HS in the ChEMBL database,³³ which is one of the largest databases on the biological activity of chemical compounds. By doing so, we do not assume that the individual components of HS can be found in ChEMBL, though we do not ascertain otherwise. Our goal was to find out what kind of chemotypes among the known natural products that possess inhibitory activity against β -lactamases might be structurally similar to those present in HS. To retrieve such compounds, we mined all inhibitors of β -lactamases reported in the ChEMBL database and selected only those that could be defined as natural-like products with at least one acidic proton in their structure, so they would be ionized using negative ESI. It is worth noting that there were only few structures retrieved with the reported activity against TEM β -lactamases, which is why we analyzed the data for β -lactamases of all molecular classes (in the SI).

In total, 306 structures corresponding to 255 unique molecular formulae were retrieved from the ChEMBL database (given in the SI). Among those, 159, 78, 1, and 17 compositions had CHO, CHON, CHOS, and CHONS elemental compositions, respectively. Figure 6 shows a van Krevelen diagram plotted for these compounds and projected onto the occupational density distributions of the molecular components, which correlated positively (highlighted in red color) and negatively (highlighted in blue color) with the activity of HS against TEM-1 β -lactamase.

It can be seen that majority of the formulae retrieved from ChEMBL populated the area with high inhibitory activity of the CHM fractions. The van Krevelen diagram resembled the population density of CHM-100-2 (the most active fraction). The compounds in this area of the van Krevelen diagram are usually attributed to flavonoid-, lignin-like structures, condensed polyphenols, and terpenoids.³¹

Although the exact mechanism of the observed inhibitory activity of the narrow apolar fractions of humatmelanic acid isolated from coal and of their combinations with β -lactam inhibitors remains unclear, several hypotheses about their mechanism of action can be suggested. The moderate inhibitory activity of apolar fractions of HS and their synergy with

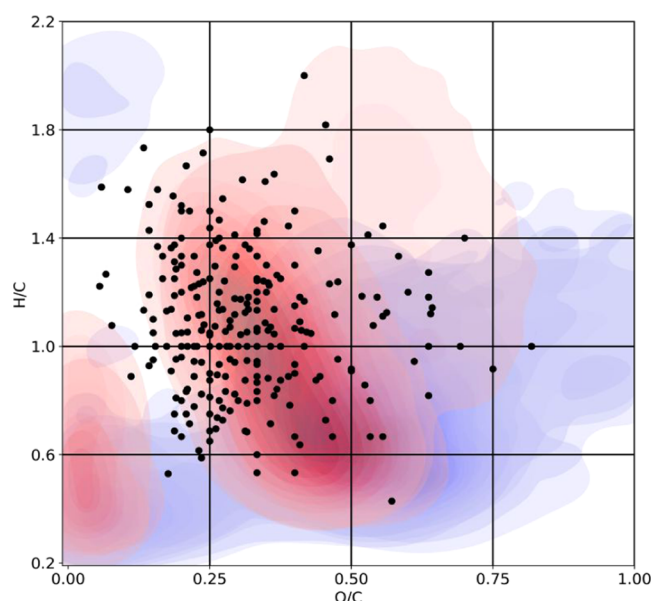


Figure 6. Van Krevelen diagram plotted for 255 unique molecular formulae of the compounds possessing inhibitory activity with regard to β -lactamases, which were retrieved from ChEMBL as matches of the molecular formulae measured by FTICR MS in CHM fractions. The background is represented by the occupation density distribution of all molecular components comprising the narrow CHM fractions, whose content correlated positively (highlighted in red) and negatively (highlighted in blue) with the inhibitory activity of these CHM fractions.

sublactam can be attributed to the preferential binding of the apolar (hydrophobic and amphiphatic) components of HS to the hydrophobic pocket of cryptic allosteric sites on the surface of the protein, which was first described by Horn and Shoichert.¹⁴ The potential presence of allosteric sites on the surface of TEM-1 β -lactamases and their influence on the active site were further investigated using laboratory experiments followed by X-ray crystallography¹⁴ and molecular dynamics simulations.^{10–13} X-ray crystallography of TEM-1 β -lactamase with different ligands showed that ligands can interact with the hidden allosteric site and disrupt the protein tertiary structure, leading to conformational changes in the active site.¹⁴ In line with this, molecular dynamics simulations showed that molecules binding to allosteric sites might affect the overall enzyme movement, causing changes in the active site, which may be related to the enzyme's ability to resist the action of particular antibiotics.¹³ In the case of HS, the interactions with allosteric sites of β -lactamase could proceed via binding of a single ligand—the specific low-molecular-weight component of HS with the allosteric site. On the other side, the colloid-like interaction of enzyme and the supramolecular aggregate of HS cannot be excluded. It was reported for quercetin (flavonoid) and gossypol (polyphenol) (retrieved among others from the ChEMBL database), which form supramolecular aggregates capable of interactions with the serine β -lactamase AmpC.^{34,35} This tendency was also observed for a large spectrum of other flavonoid-like compounds.^{36–40} Given the same inhibition kinetics, which was observed in the control experiments on the possibility of adduct formation between the HS and CENTA, as well as between TEM-1 β -lactamase and hydrolyzed CENTA (Tables S7–S9), the colloidal mechanism looks less probable, but it cannot be neglected in further studies on the molecular mechanisms of inhibition of β -lactamase by HS.

CONCLUSIONS

The presented study for the first time demonstrated that the natural HS possessed inhibitory activity with regard to the TEM-1 β -lactamase. Moreover, it has shown a way for enhancing this activity by directed isolation of the apolar (hydrophobic and amphiphatic) components of the humic ensemble using SPE extraction and gradient elution. A novel approach to the generation of quantitative descriptors for the molecular composition of HS was tested by deriving them from the population density distribution of the molecular components of HS in the van Krevelen diagram. It has demonstrated good prospects for building molecular composition–activity relationships and can be easily extended to other HS and natural complex matrices in general. The undertaken chemoinformatic study allowed us to suggest that the inhibitory activity of HS with respect to β -lactamase might be connected both to the interaction of the single low-molecular-weight components of HS with the cryptic allosteric site of β -lactamase and to the nonspecific interaction of the supramolecular aggregate of HS components with the surface of the protein, which bring about a change in the conformation of the active site. Further studies on HS from different natural sources and their fractions obtained with using much finer separation technologies (e.g., two-dimensional (2D) chromatography) might bring substantial advancement in the field of directed design of humic-based materials for fighting antibacterial resistance.

EXPERIMENTAL SECTION

Reagents and the Parent Humic Materials Used in This Study. Substrate and Inhibitors. Chromogenic β -lactamase substrate CENTA (CAS 9073-60-3, 98%),⁴¹ sublactam (99%), and tazobactam (99%) were purchased from Sigma-Aldrich (Germany).

Enzyme. Recombinant β -lactamase TEM-1 was expressed in *Escherichia coli* and purified as described by Grigorenko et al.¹⁷ In brief, the recombinant enzyme was isolated from bacterial periplasm using the osmotic shock procedure and purified further by anion-exchange and size exclusion chromatography. Two batches of TEM-1 corresponding to different isolations (isolation procedure was the same) were used in concentrations of 17 and 10 nM in the experiments on the inhibitory activity of HS from different sources (Figure 1).

Humic Materials. The set of humic materials included the potassium humate (CHP) provided by Humintech Ltd. (Grevenbroich, Germany) under the trade name Powhumus, a commercial sample of potassium/sodium humate “Humate-Extra” (CHI), soil humic acids (SHA), peat humic acids collected from The Great Vasyugan Mire (PHA), and humatomelanolic acids (CHM), previously isolated from CHI using ethanol extraction as described by Stevenson.⁴² The data on the elemental and structural-group compositions of the humic materials are summarized in Table S1 of the Supporting Information. The ¹³C NMR spectra for both humic materials are shown in Figure S1 of the Supporting Information.

SPE-Fractionation of the CHM Sample Using Gradient Elution. The narrow fractions of CHM were obtained using sorption on a Bond Elut PPL SPE cartridge (100 mg, 3 mL) (Agilent Technologies) followed by gradient elution with water:methanol mixtures. The PPL SPE cartridge was activated by passing 3 mL of methanol immediately prior to fractionation as described by Dittmar et al. and Zhrebek et al.^{43,44} CHM solution (300 mL of 207 mg·L⁻¹) was pre-acidified with 1 M

HCl to pH 2.0 and discharged through the cartridge. Then, the cartridge was washed with 3 mL of 0.01 M HCl for complete elimination of salts and dried for 30 min in the air flow. The CHM fractions were then eluted by passing equal portions (10 mL) of water/methanol solutions at 2 mL·min⁻¹ flow rate. The following MeOH/H₂O ratios (v/v) were used: 10:90, 20:80, 30:70, 40:60, 50:50, 60:40, 80:20, 100:0 (the first portion), and 100:0 (the second portion). Two portions of pure methanol were used to ensure full recovery of the sorbed humic material. The collected eluates were evaporated to dryness in vacuo and re-dissolved in 50 mM sodium phosphate buffer, pH 7.0 at 25 °C. Masses of the recovered fractions are given in Table S2 of the Supporting Information.

Determination of Catalytic Parameters of β -Lactamase TEM-1. The catalytic activity of β -lactamase TEM-1 was determined in the hydrolysis reaction of chromogenic substrate CENTA—structural analogue of antibiotic cephalothin described by Bebrone et al.⁴¹ The stock solution of CENTA (1 mM) was prepared in 50 mM sodium phosphate buffer, pH 7.0. Assay conditions: 50 mM sodium phosphate buffer pH 7.0, 25 °C, enzyme concentration of 17 nM. The reaction was initiated by adding the substrate solution to the enzyme-containing solution. The hydrolysis of CENTA was monitored by continuous recording of the absorbance at 405 nm ($\epsilon_{405} = 6400 \text{ M}^{-1}\cdot\text{cm}^{-1}$) for 3 min.

Catalytic parameters of the β -lactamase hydrolysis were determined using different concentrations of CENTA (10, 20, 30, and 50 μM). The measurements were made in triplicates. Initial hydrolysis rates were determined from the slopes of the initial intersects of the kinetic curves for a period of 10 s. The values of Michaelis constant (K_M) and V_{max} were determined using the weighted Lineweaver–Burk and Eadie–Hofstee linearization (Figure S2a,b). The K_M values determined in the Lineweaver–Burk and Eadie–Hofstee coordinates accounted for 25.2 and 22.0 μM ; the values of the maximum reaction rate (V_{max}) were 0.43 and 0.39 $\mu\text{M}\cdot\text{s}^{-1}$, respectively, which agreed well with the reported earlier data for the narrow-spectrum TEM-type β -lactamase measured under the same experimental conditions.¹⁷

Control experiments on the possibility of adduct formation between the HS and CENTA, as well as between TEM-1 β -lactamase and hydrolyzed CENTA, were performed using UV–vis spectroscopy. The details are given in the Supporting Information (Tables S7 and S8 and Figure S4).

Study of Individual and Combined Action of HS and β -Lactam Inhibitors on β -Lactamase TEM-1. β -Lactam inhibitors (sulbactam and tazobactam) and HS were added to the enzyme/substrate mixture in 50 mM sodium phosphate buffer, pH 7.0, separately and in combination. The concentrations of stock solutions of CENTA, β -lactamase TEM-1, sulbactam, tazobactam, and HS (CHP, CHI, SHA, PHA, CHM, and the fractions of CHM) are given in Table 5. The total assay volume was 3 mL. The reaction was initiated by adding the required aliquot of enzyme stock solution to the mixture of the reagents. The kinetic curves of the accumulation of the CENTA hydrolysis product were recorded by absorbance at 405 nm during 30 min. The intrinsic optical absorption of HS was automatically subtracted, since it does not introduce significant errors in the kinetics determinations (the details are provided in the Supporting Information, Table S9).

The following humic materials were used in the inhibition assays: CHP, CHM, and all narrow CHM fractions. Combined

Table 5. Reagent Concentrations in the Experiments on Inhibition of β -Lactamase TEM-1 by HS and β -Lactam Inhibitors

	stock solution concentration	aliquot (μL)	concentration in the reaction mixture
CENTA	1 mM	300	100 μM
β -lactamase TEM-1	34/0.85 μM	1.5/35	17/10 nM
sulbactam	2 mM	7.5	5 μM
tazobactam	0.2 mM	7.5	0.5 μM
HS sample	200 $\text{mg}\cdot\text{L}^{-1}$	750	50 $\text{mg}\cdot\text{L}^{-1}$

inhibition with sulbactam and tazobactam was studied with the use of CHP, CHM, CHM-50, CHM-100-1, and CHM-100-2.

The relative decrease in the initial rate of CENTA hydrolysis by β -lactamase TEM-1 in the presence of CHM fractions was calculated according to eq 1

$$\text{RI} = \left(1 - \frac{v_1}{v_0} \right) \times 100\% \quad (1)$$

where v_1 is the initial rate of the hydrolysis reaction in the presence of inhibitor (HS, β -lactam inhibitor, or both of them), and v_0 is the initial rate of the uninhibited hydrolysis reaction.

Data Treatment of the Inhibition Experiments with a Combination of Low-Molecular-Weight β -Lactam Inhibitors and Humic Inhibitors. The initial rates of CENTA hydrolysis were determined as slopes of kinetic curves over the first 3 min of reaction. The combined action of two types of inhibitors was compared with their separate action using the additive model of the action of two inhibitors according to eq 2²⁶

$$1/v_{1,2} = 1/v_1 + 1/v_2 - 1/v_0 \quad (2)$$

where v_1 , v_2 are the initial rates of CENTA hydrolysis in the presence of inhibitor 1 (β -lactam inhibitor sulbactam or tazobactam) and inhibitor 2 (HS), v_0 is the initial velocity of the uninhibited reaction of CENTA hydrolysis, and $v_{1,2}$ is the initial velocity in the presence of the mixture of inhibitors 1 and 2.

If the calculated value $v_{1,2}$ was higher than the experimentally determined ones, then the conclusion was made on the synergistic effect of the HS and β -lactam inhibitors on CENTA hydrolysis. If the calculated value $v_{1,2}$ was lower than the experimental ones, the conclusion was made on the antagonistic effect of two inhibitors. If the calculated and experimental initial rates $v_{1,2}$ were equal, then a decrease in the initial reaction rate could be related exclusively to an increase in the concentration of inhibitors, which is indicative of the additive effect of the inhibitors.

FTICR MS Analysis of the Humic Materials. FTICR MS analysis of the HS samples was performed using an FT MS spectrometer Bruker Apex Ultra (Bruker Daltonics) equipped with a dynamically harmonized cell, a 7 T superconducting magnet, and an electrospray ionization (ESI) source. Each of the mass spectra were acquired in negative ionization mode by direct infusion at a flow rate of 120 $\text{mL}\cdot\text{h}^{-1}$ by summarizing 400 scans. The internal calibration of the obtained mass spectra was systematically conducted using the known peak series of HS, reaching accuracy values of <0.5 ppm. Mass lists were created using Data Analysis 3.4 software (Bruker Daltonics). Molecular assignments were made using lab-made Transhumus software. Ion charge was directly determined for abundant peaks using the m/z difference between ¹³C and ¹²C isotopologues, and was

extended for minor peaks using the total mass differences algorithm.⁴⁵ Formulae were filtered using the following typical atomic constraints: O/C ≤ 1, H/C ≤ 2.2, C ≤ 120, H ≤ 200, 0 < O ≤ 60, and N ≤ 2, S ≤ 1.

Establishing Molecular Composition–Activity Relationships for the Inhibitory Activity of the HS Fractions.

For the narrow fractions of CHM, the relationships were established between molecular composition and inhibitory activity with respect to β -lactamase. The descriptors of molecular composition of HS were determined as described by Perminova.⁵¹ They were generated by binning the van Krevelen diagram into 20 cells and calculating the intensity-weighted population density of each cell using the following equation

$$D_k = \frac{\sum_{i=1}^{N_k} I_i}{\sum_{j=1}^N I_j}, k = 1, 2 \dots N \quad (3)$$

where D_k is the intensity-weighted population density of the cell k ; N is the total number of points in the diagram; N_k is the number of points belonging to the cell k ; I_j is the intensity of point j ; and I_i is the point i belonging to the cell k peak intensity.

The obtained matrix was used for correlation analysis with the corresponding data on the inhibitory activity of each fraction. Multiple regression was used to construct the composition–activity relationships for the obtained data sets.

ChEMBL Data Mining. The following procedures were used to retrieve the data from ChEMBL. The MySQL version of ChEMBL (v. 26) database was downloaded from ChEMBL ftp web service and set up on a local MySQL server.⁴⁶ The data on the activities, assays, and compound structures tested against β -lactamases were retrieved and processed using a set of MySQL queries and text mining procedures implemented as a Python script. At first, all entries from the *target_dictionary* table containing the “pref_name” field matching the regular expression “ β (.*)lactamase” were retrieved. Data on the activities, descriptions of assays, and structures of compounds were then retrieved from the *activities*, *assays*, *compound_structures* table using “tid” values from the *target_dictionary* table as keys. Additional assays related to TEM-1 β -lactamase were also searched in the “description” field of the *assays* table using the regular expression “TEM-1(0,1)1(\\D)”. The retrieved entries were manually curated to keep only the relevant ones and added to the data set. The entries were also filtered by activity values: all entries for which the “pchembl_value” field was empty or the “activity_comment” field contained values “Not Active” or “inactive” were filtered out. The structures of the compounds (canonical_smiles field from the *compound_structures* table) were standardized using the following procedures: (1) smiles strings were split by the “.” symbol and the largest substring consisting of alphabetic symbols was kept; (2) compounds were uncharged, and stereochemistry was removed using the RDKit library. Formulae corresponding to standardized structures were matched to formulae from HS samples. pKa values were calculated using OPERA software.⁴⁷ The natural product likeness (NPLike) score was calculated according to P. Ertl’s approach using RDKit library.^{48,49} Only the compounds with NPLike score values larger than 0 and the ones containing at least one acidic proton (COOH, AlkOH, or ArOH groups) were kept in the data set.

■ ASSOCIATED CONTENT

Supporting Information

The Supporting Information is available free of charge at <https://pubs.acs.org/doi/10.1021/acsomega.1c02841>.

Elemental and structural-group compositions of the parent humic materials (Table S1) and corresponding ¹³C NMR spectra (Figure S1); experimental data on the CENTA hydrolysis by β -lactamase TEM-1 (Figure S2); kinetic curves of CENTA hydrolysis by β -lactamase TEM-1 in the presence of narrow fractions of CHM (Figure S3); the data on yield of the narrow CHM fractions eluted from the SPE PPL cartridge (Table S2); correlation of molecular composition of CHM fractions expressed with occupational density descriptors and their inhibitory activity (Table S3), regression relationships for molecular composition and inhibitory activity of the CHM fractions (Tables S4–S6); optical density of the enzyme solution at a wavelength of 405 nm in the presence of CHM (Table S7); kinetic curves of CENTA hydrolysis by β -lactamase TEM-1 in presence of CHM with/without preliminary centrifugation of CHM with TEM-1 (Figure S4); optical density of the solution of the hydrolysis product at a wavelength of 405 nm in the presence of CHP (Table S8); the absolute values of intrinsic optical absorption of CHP and CHM (A_{HS}) and the observed increase in optical density due to the hydrolysis of CENTA (ΔA_{405}) in presence of CHP and CHM in the same concentrations (Table S9) (PDF)

FTICR MS data with assigned molecular formulae of the CHM fractions and the data on smiles, biological activity, number of acidic protons and natural product likeness, enclosed on 306 structures retrieved from the ChEMBL database (XLS)

■ AUTHOR INFORMATION

Corresponding Author

Irina V. Perminova – Department of Chemistry, Lomonosov Moscow State University, Moscow 119991, Russia;
orcid.org/0000-0001-9084-7851; Email: iperm@med.chem.msu.ru; Fax: +7 495 939 5546

Authors

Tatyana A. Mikhnevich – Department of Chemistry, Lomonosov Moscow State University, Moscow 119991, Russia
Alexandra V. Vyatkina (Turkova) – Department of Chemistry, Lomonosov Moscow State University, Moscow 119991, Russia
Vitaly G. Grigorenko – Department of Chemistry, Lomonosov Moscow State University, Moscow 119991, Russia
Maya Yu. Rubtsova – Department of Chemistry, Lomonosov Moscow State University, Moscow 119991, Russia;
orcid.org/0000-0003-4025-5967
Gleb D. Rukhovich – Department of Chemistry, Lomonosov Moscow State University, Moscow 119991, Russia
Maria A. Letarova – Vinogradsky Institute of Microbiology, RC Biotechnology of RAS, Moscow 117312, Russia
Darya S. Kravtsova – Department of Chemistry, Lomonosov Moscow State University, Moscow 119991, Russia
Sergey A. Vladimirov – Department of Chemistry, Lomonosov Moscow State University, Moscow 119991, Russia
Alexey A. Orlov – Skolkovo Institute of Science and Technology, Moscow 121205, Russia; Present Address: Universite de

Strasbourg 4, rue B. Pascal, Strasbourg, FR 67000, France;

orcid.org/0000-0002-0597-7705

Evgeny N. Nikolaev – Skolkovo Institute of Science and Technology, Moscow 121205, Russia; orcid.org/0000-0001-6209-2068

Alexander Zhrebker – Skolkovo Institute of Science and Technology, Moscow 121205, Russia; orcid.org/0000-0002-3481-4606

Complete contact information is available at:

<https://pubs.acs.org/10.1021/acsomega.1c02841>

Notes

The authors declare no competing financial interest.

ACKNOWLEDGMENTS

The authors appreciate the partial support supported by the grants of the Russian Science Foundation as part of the narrow fractions isolation and evaluation of their inhibitory activity with regard to TEM-1 β -lactamase (20-63-47070) and their FTICR MS measurements (21-47-04405). These studies were conducted in the framework of the Scientific-Educational School of the Lomonosov MSU “Future of the planet and global change in the environment”.

REFERENCES

- (1) Watkins, R. R.; Bonomo, R. A. Overview: Global and Local Impact of Antibiotic Resistance. *Infect. Dis. Clin. North Am.* **2016**, *30*, 313–322.
- (2) Smith, R. A.; M'ikanatha, N. M.; Read, A. F. Antibiotic Resistance: A Primer and Call to Action. *Health Commun.* **2015**, *30*, 309–314.
- (3) Hughes, D.; Andersson, D. I. Evolutionary Trajectories of Antibiotic Resistance. *Annu. Rev. Microbiol.* **2017**, *71*, 579–596.
- (4) Klein, E. Y.; Van Boeckel, T. P.; Martinez, E. M.; Pant, S.; Gandra, S.; Levin, S. A.; Goossens, H.; Laxminarayan, R. Global Increase and Geographic Convergence in Antibiotic Consumption between 2000 and 2015. *Proc. Natl. Acad. Sci. U.S.A.* **2018**, *115*, E3463–E3470.
- (5) Bush, K. Past and Present Perspectives on β -Lactamases. *Antimicrob. Agents Chemother.* **2018**, *62*, 1076.
- (6) Drawz, S. M.; Bonomo, R. A. Three Decades of β -Lactamase Inhibitors. *Clin. Microbiol. Rev.* **2010**, *23*, 160–201.
- (7) Tooke, C. L.; Hinchliffe, P.; Bragginton, E. C.; Colenso, C. K.; Hirvonen, V. H. A.; Takebayashi, Y.; Spencer, J. β -Lactamases and β -Lactamase Inhibitors in the 21st Century. *J. Mol. Biol.* **2019**, *431*, 3472–3500.
- (8) Noguchi, T.; Matsumura, Y.; Kanahashi, T.; Tanaka, M.; Tsuchido, Y.; Matsumura, T.; Nakano, S.; Yamamoto, M.; Nagao, M.; Ichiyama, S. Role of TEM-1 β -Lactamase in the Predominance of Ampicillin-Sulbactam-Nonsusceptible *Escherichia Coli* in Japan. *Antimicrob. Agents Chemother.* **2019**, *63*, No. 2366.
- (9) Krizova, L.; Poirel, L.; Nordmann, P.; Nemeč, A. TEM-1 β -Lactamase as a Source of Resistance to Sulbactam in Clinical Strains of *Acinetobacter baumannii*. *J. Antimicrob. Chemother.* **2013**, *68*, 2786–2791.
- (10) Bowman, G. R.; Geissler, P. L. Equilibrium fluctuations of a single folded protein reveal a multitude of potential cryptic allosteric sites. *Proc. Natl. Acad. Sci. U.S.A.* **2012**, *109*, 11681–11686.
- (11) Bowman, G. R.; Bolin, E. R.; Hart, K. M.; Maguire, B. C.; Marqusee, S. Multiple hidden allosteric sites. *Proc. Natl. Acad. Sci. U.S.A.* **2015**, *112*, 2734–2739.
- (12) Avci, F. G.; Altinsik, F. E.; Ulu, D. V.; Olmez, E. O.; Akbulut, B. S. An evolutionarily conserved allosteric site modulates beta-lactamase activity. *J. Enzyme Inhib. Med. Chem.* **2016**, *31*, 33–40.
- (13) Avci, F. G.; Altinsik, F. E.; Karacan, I.; Karagoz, D. S.; Ersahin, S.; Eren, A.; Sayar, N. A.; Ulu, D. V.; Ozkirimli, E.; Akbulut, B. S. Targeting a hidden site on class A beta-lactamases. *J. Mol. Graphics Modell.* **2018**, *84*, 125–133.
- (14) Horn, J. R.; Shoichet, B. K. Allosteric Inhibition Through Core Disruption. *J. Mol. Biol.* **2004**, *336*, 1283–1291.
- (15) Galdadas, I.; Qu, S.; Oliveira, A. S. F.; Olehnovics, E.; Mack, A. R.; Mojica, M. F.; Agarwal, P. K.; Tooke, C. L.; Gervasio, F. L.; Spencer, J.; Bonomo, R. A.; Mulholland, A. J.; Haider, S. Allosteric communication in class A β -lactamases occurs via cooperative coupling of loop dynamics. *eLife* **2021**, *10*, No. 66567.
- (16) Ghattas, M. A.; Al Rawashdeh, S.; Atatreh, N.; Bryce, R. A. How do small molecule aggregates inhibit enzyme activity? A molecular dynamics study. *J. Chem. Inf. Model.* **2020**, *60*, 3901–3909.
- (17) Grigorenko, V. G.; Andreeva, I. P.; Rubtsova, M. Y.; Deygen, I. M.; Antipin, R. L.; Majouga, A. G.; Egorov, A. M.; Beshnova, D. A.; Kallio, J.; Hackenberg, C.; Lamzin, V. S. Novel Non- β -Lactam Inhibitor of β -Lactamase TEM-171 Based on Acylated Phenoxyaniline. *Biochimica* **2017**, *132*, 45–53.
- (18) Pemberton, O. A.; Jaishankar, P.; Akhtar, A.; Adams, J. L.; Shaw, L. N.; Renslo, A. R.; Chen, Y. Heteroaryl Phosphonates as Noncovalent Inhibitors of Both Serine- and Metallo-carboxypeptidases. *J. Med. Chem.* **2019**, *62*, 8480–8496.
- (19) Piccolo, A. The Supramolecular Structure of Humic Substances. *Soil Sci.* **2001**, *166*, 810–832.
- (20) Tomaszewski, J. E.; Schwarzenbach, R. P.; Sander, M. Protein Encapsulation by Humic Substances. *Environ. Sci. Technol.* **2011**, *45*, 6003–6010.
- (21) Tan, W. F.; Koopal, L. K.; Norde, W. Interaction between Humic Acid and Lysozyme, Studied by Dynamic Light Scattering and Isothermal Titration Calorimetry. *Environ. Sci. Technol.* **2009**, *43*, 591–596.
- (22) Li, Y.; Tan, W.; Koopal, L. K.; Wang, M.; Liu, F.; Norde, W. Influence of Soil Humic and Fulvic Acid on the Activity and Stability of Lysozyme and Urease. *Environ. Sci. Technol.* **2013**, *47*, 5050–5056.
- (23) Giachin, G.; Narkiewicz, J.; Scaini, D.; Ngoc, A. T.; Margon, A.; Sequi, P.; Leita, L.; Legname, G. Prion Protein Interaction with Soil Humic Substances: Environmental Implications. *PLoS One* **2014**, *9*, No. e100016.
- (24) Sarkar, J. M.; Bollag, J. M. Inhibitory Effect of Humic and Fulvic Acids on Oxidoreductases as Measured by the Coupling of 2,4-Dichlorophenol to Humic Substances. *Sci. Total Environ.* **1987**, *62*, 367–377.
- (25) Fulvic Acid and Antibiotic Combination for the Inhibition or Treatment of Multidrug Resistant Bacteria. US2015/0031767.
- (26) Chou, T. C.; Talalay, P. A Simple Generalized Equation for the Analysis of Multiple Inhibitions of Michaelis-Menten Kinetic Systems. *J. Biol. Chem.* **1977**, *252*, 6438–6442.
- (27) Uporov, I. V.; Grigorenko, V. G.; Rubtsova, M. Y.; Egorov, A. M. Molecular Dynamics Study of the Complex Formation of TEM-Type β -Lactamases with Substrates and Inhibitors. *Moscow Univ. Chem. Bull.* **2018**, *73*, 27–33.
- (28) Nebbiosio, A.; Piccolo, A.; Spittler, M. Limitations of Electrospray Ionization in the Analysis of a Heterogeneous Mixture of Naturally Occurring Hydrophilic and Hydrophobic Compounds. *Rapid Commun. Mass Spectrom.* **2010**, *24*, 3163–3170.
- (29) Rodgers, R. P.; Mapolelo, M. M.; Robbins, W. K.; Chacón-Patiño, M. L.; Putman, J. C.; Niles, S. F.; Rowland, S. M.; Marshall, A. G. Combating Selective Ionization in the High-Resolution Mass Spectral Characterization of Complex Mixtures. *Faraday Discuss.* **2019**, *218*, 29–51.
- (30) Zhrebker, A.; Shirshin, E.; Rubekina, A.; Kharybin, O.; Kononikhin, A.; Kulikova, N. A.; Zaitsev, K. V.; Roznyatovsky, V. A.; Grishin, Y. K.; Perminova, I. V.; Nikolaev, E. N. Optical Properties of Soil Dissolved Organic Matter Are Related to Acidic Functions of Its Components as Revealed by Fractionation, Selective Deuteromethylation, and Ultrahigh Resolution Mass Spectrometry. *Environ. Sci. Technol.* **2020**, *54*, 2667–2677.
- (31) Perminova, I. V. From Green Chemistry and Nature-like Technologies towards Ecoadaptive Chemistry and Technology. *Pure Appl. Chem.* **2019**, *91*, 851–864.
- (32) Orlov, A. A.; Zhrebker, A.; Eletskaia, A. A.; Chernikov, V. S.; Kozlovskaya, L. I.; Zhernov, Y. V.; Kostyukovich, Y.; Palyulin, V. A.;

Nikolaev, E. N.; Osolodkin, D. I.; Perminova, I. V. Examination of Molecular Space and Feasible Structures of Bioactive Components of Humic Substances by FTICR MS Data Mining in ChEMBL Database. *Sci. Rep.* **2019**, *9*, No. 12066.

(33) Gaulton, A.; Hersey, A.; Nowotka, M. L.; Patricia Bento, A.; Chambers, J.; Mendez, D.; Mutowo, P.; Atkinson, F.; Bellis, L. J.; Cibrian-Uhalte, E.; Davies, M.; Dedman, N.; Karlsson, A.; Magarinos, M. P.; Overington, J. P.; Papadatos, G.; Smit, I.; Leach, A. R. The ChEMBL Database in 2017. *Nucleic Acids Res.* **2017**, *45*, D945–D954.

(34) McGovern, S. L.; Helfand, B. T.; Feng, B.; Shoichet, B. K. A Specific Mechanism of Nonspecific Inhibition. *J. Med. Chem.* **2003**, *46*, 4265–4272.

(35) Feng, B. Y.; Simeonov, A.; Jadhav, A.; Babaoglu, K.; Inglese, J.; Shoichet, B. K.; Austin, C. P. A High-Throughput Screen for Aggregation-Based Inhibition in a Large Compound Library. *J. Med. Chem.* **2007**, *50*, 2385–2390.

(36) Pohjala, L.; Tammela, P. Aggregating Behavior of Phenolic Compounds - A Source of False Bioassay Results? *Molecules* **2012**, *17*, 10774–10790.

(37) Osonga, F. J.; Akgul, A.; Miller, R. M.; Eshun, G. B.; Yazgan, I.; Akgul, A.; Sadik, O. A. Antimicrobial Activity of a New Class of Phosphorylated and Modified Flavonoids. *ACS Omega* **2019**, *4*, 12865–12871.

(38) Górniak, I.; Bartoszewski, R.; Króliczewski, J. Comprehensive Review of Antimicrobial Activities of Plant Flavonoids. *Phytochem. Rev.* **2019**, *18*, 241–272.

(39) Budzyńska, A.; Wickowska-Szakiel, M.; Sadowska, B.; Rozalska, B.; Rozalski, M.; Karolczak, W. Synthetic 3-Arylidene flavanones as Inhibitors of the Initial Stages of Biofilm Formation by *Staphylococcus aureus* and *Enterococcus faecalis*. *Z. Naturforsch., C* **2011**, *66*, 104–114.

(40) Vikram, A.; Jayaprakasha, G. K.; Jesudhasan, P. R.; Pillai, S. D.; Patil, B. S. Suppression of Bacterial Cell-Cell Signalling, Biofilm Formation and Type III Secretion System by Citrus Flavonoids. *J. Appl. Microbiol.* **2010**, *109*, 515–527.

(41) Bebrone, C.; Moali, C.; Mahy, F.; Rival, S.; Docquier, J. D.; Rossolini, G. M.; Fastrez, J.; Pratt, R. F.; Frère, J. M.; Galleni, M. CENTA as a Chromogenic Substrate for Studying β -Lactamases. *Antimicrob. Agents Chemother.* **2001**, *45*, 1868–1871.

(42) Stevenson, F. Geochemistry of Soil Humic Substances. In *Humic Substances in Soil, Sediment, and Water*; Aiken, G. R.; McKnight, D. M.; Wershaw, R. L.; MacCarthy, P., Eds.; John Wiley & Sons, 1985; pp 13–52.

(43) Dittmar, T.; Koch, B.; Hertkorn, N.; Kattner, G. A Simple and Efficient Method for the Solid-Phase Extraction of Dissolved Organic Matter (SPE-DOM) from Seawater. *Limnol. Oceanogr. Methods* **2008**, *6*, 230–235.

(44) Zhrebek, A.; Kostyukevich, Y.; Kononikhin, A.; Kharybin, O.; Konstantinov, A. I.; Zaitsev, K. V.; Nikolaev, E.; Perminova, I. V. Enumeration of Carboxyl Groups Carried on Individual Components of Humic Systems Using Deuteromethylation and Fourier Transform Mass Spectrometry. *Anal. Bioanal. Chem.* **2017**, *409*, 2477–2488.

(45) Kunenkov, E. V.; Kononikhin, A. S.; Perminova, I. V.; Hertkorn, N.; Gaspar, A.; Schmitt-Kopplin, P.; Popov, I. A.; Garmash, A. V.; Nikolaev, E. N. Total Mass Difference Statistics Algorithm: A New Approach to Identification of High-Mass Building Blocks in Electrospray Ionization Fourier Transform Ion Cyclotron Mass Spectrometry Data of Natural Organic Matter. *Anal. Chem.* **2009**, *81*, 10106–10115.

(46) ChEMBL ftp web-service ftp://ftp.ebi.ac.uk/pub/databases/chembl/ChEMBLdb/releases/chembl_26/ (accessed Jan, 2021).

(47) Mansouri, K.; Grulke, C. M.; Judson, R. S.; Williams, A. J. OPERA Models for Predicting Physicochemical Properties and Environmental Fate Endpoints. *J. Cheminf.* **2018**, *10*, No. 10.

(48) Ertl, P.; Roggo, S.; Schuffenhauer, A. Natural Product-Likeness Score and Its Application for Prioritization of Compound Libraries. *J. Chem. Inf. Model.* **2008**, *48*, 68–74.

(49) RDKit: Open-source cheminformatics; <http://www.rdkit.org/> (accessed Jan, 2021).